Journal of Ceramic Processing Research. Vol. 19, No. 5, pp. 434~438 (2018)

J O U R N A L O F
Ceramic Processing Research

Use of copper tungsten oxide as a liquid phase sintering aid for barium hexaferrite

John G. Fisher*, Phan Gia Le, Meng Meng, Sang-Hyeon Heo, Tae-Jin Bak, Byeol-Lee Moon, In-San Park, Dong-Kyu Lee and Wu-Hui Lee

School of Materials Science and Engineering, Chonnam National University, Gwangju 61186, Republic of Korea

The sintering behavior of $BaFe_{12}O_{19}$ with the addition of one and three weight % of $CuWO_4$ as a liquid phase sintering aid is studied. Samples are sintered in the temperature range 900-1250 °C and the effect of $CuWO_4$ addition on density, microstructure, phase composition and magnetic properties is examined. Compared to $BaFe_{12}O_{19}$ with no sintering aid addition, addition of 1 wt % $CuWO_4$ retards densification. Addition of 3 wt % $CuWO_4$ promotes densification at lower sintering temperatures but retards densification at temperatures > 1050 °C. Three wt % $CuWO_4$ addition induces the formation of $BaWO_4$ and $Ba_3WFe_2O_9$ secondary phases at temperatures ≥ 1100 °C. Addition of $CuWO_4$ causes a decrease in saturation magnetization, remanent magnetization and coercivity.

Key words: Ferrites, Magnetic properties, Liquid phase sintering, Microstructure, Hard magnets.

Introduction

Barium hexaferrite, $BaFe_{12}O_{19}$, a hard ferrimagnetic material which finds many uses e.g. as permanent magnets, in recording media and in microwave applications [1-3], is usually sintered at temperatures between 1200-1300 °C [4]. Reduction of the sintering temperature would be beneficial in reducing production costs and expanding the range of applications for this material. For example, for low temperature co-fired ceramic applications, the sintering temperature should be lowered to 900 °C [5-7]. The use of a liquid phase sintering aid is an effective strategy to lower the sintering temperature of $BaFe_{12}O_{19}$. Several workers have used liquid phase sintering aids such as CuO, $BaCuO_2$, Bi_2O_3-B_2O_3-SiO_2-ZnO glass powder and Bi_2O_3 to reduce the sintering temperature to within the range 900 °C-1100 °C [4, 6, 8]. However, addition of a liquid phase sintering aid may result in abnormal grain growth, which can be detrimental to the mechanical and magnetic properties [4, 6].

The current work looks at the use of $CuWO_4$ as a liquid phase sintering aid for $BaFe_{12}O_{19}$. $CuWO_4$ is antiferromagnetic below –250 °C [9] and has a melting point of ~1000 °C [10]. Its use as a sintering aid does not appear in the literature to our knowledge. Its low melting point may make it suitable as a sintering aid.

*Corresponding author:
Tel : +82-62-530-1702
Fax: +82-62-530-1699
E-mail: johnfisher@jnu.ac.kr

Experimental

A commercial $BaFe_{12}O_{19}$ powder (99.2%, supplied by LG Innotek Co. Ltd.) was used. The powder was dried at 250 °C for 1 hr to remove adsorbed water. To prepare the $BaFe_{12}O_{19}$ powder without sintering aid addition, 30 g of powder was weighed and then ball milled in high purity ethanol (99.9%) with zirconia media in a polypropylene jar for 24 hrs. After evaporating the ethanol with a hot plate and stirrer, the powder was ground in an agate mortar and pestle and sieved to pass a 180 μm mesh. To prepare the powder with sintering aid addition, $BaFe_{12}O_{19}$ powder and $CuWO_4$ powder (99.5%, Alfa Aesar) were dried at 250 °C for 1 hr, weighed, ball milled, ground and sieved as above. The compositions of the sintering aid - added powders are 99 wt% $BaFe_{12}O_{19}$-1 wt% $CuWO_4$ and 97 wt% $BaFe_{12}O_{19}$-3 wt% $CuWO_4$.

Powders were pressed by hand in a stainless steel die of 10 mm diameter to form pellet-shaped samples. The samples were then cold isostatically pressed at a pressure of 1500 kgf (147 MPa). Samples were sintered in the temperature range 900-1250 °C for 1 h with heating and cooling rate of 5 °C.min^{-1}. To reduce Ba volatilization, samples were buried in $BaFe_{12}O_{19}$ packing powder in a double alumina crucible with lids.

The density of sintered samples was measured via the Archimedes principle in deionized water. The phase structure of selected samples was investigated by X-ray diffraction (XRD) with Cu K_α radiation (XRD XPert PRO, PANalytical, The Netherlands) with $2\theta = 20$ °-80 °, scan speed = 3 °.min^{-1} and 0.02 ° step size. Unit cell parameters were calculated from the XRD patterns by the least-squares method using the program Jade 6.5 (Materials Data Inc., CA). Samples were vertically

sectioned using a low speed diamond wheel saw, polished to a 1 μm finish and thermally etched. Samples were Pt coated and the microstructure analyzed using scanning electron microscopy (SEM, Hitachi S-4700 FE-SEM, Hitachi High-Tech, Tokyo, Japan) with an attached energy dispersive spectrometer using standardless quantification (EDS, EMAX Energy EX-200, Horiba, Kyoto, Japan). Magnetic hysteresis loops were measured at room temperature using a vibrating sample magnetometer (VSM, Lake Shore VSM 704, Westerville, OH).

Results

The Archimedes density of the sintered samples is shown in Fig. 1. The density of the $BaFe_{12}O_{19}$ samples increases with sintering temperature, reaching a maximum value of 94% theoretical density at 1200 ºC before decreasing slightly at 1250 ºC. Addition of 1 wt % $CuWO_4$ has no effect on density in the temperature range 900-950 ºC, causes a small increase in density in the temperature range 1000-1050 ºC and a noticeable decrease in density in the temperature range 1100-1200 ºC. Sintered density reaches a value comparable with the $BaFe_{12}O_{19}$ samples at 1250 ºC. Addition of 3 wt % $CuWO_4$ causes a moderate increase in density of samples sintered in the range 900-1050 ºC, but a small decrease in density in the range 1100-1200 ºC. Samples from all three compositions have the same density value at 1250 ºC.

SEM micrographs of the $BaFe_{12}O_{19}$ samples sintered at temperatures between 900-1250 ºC for 1 hr are shown in Fig. 2. The samples consist mainly of equiaxed matrix grains. The matrix grain size is initially submicron and increases with increasing sintering temperature, becoming micron-sized at 1200 and 1250 ºC. Samples sintered at 950-1000 ºC are still in the initial stage of sintering, with little formation of grain boundaries between the powder particles. Samples sintered at 1050 and 1100 ºC are in

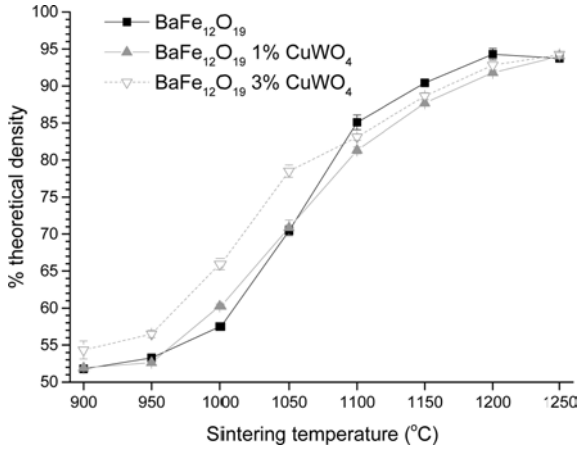

Fig. 1. Archimedes density of the $BaFe_{12}O_{19}$, 99 wt% $BaFe_{12}O_{19}$-1 wt% $CuWO_4$ and 97 wt% $BaFe_{12}O_{19}$-3 wt% $CuWO_4$ samples sintered at 900-1250 ºC for 1 h.

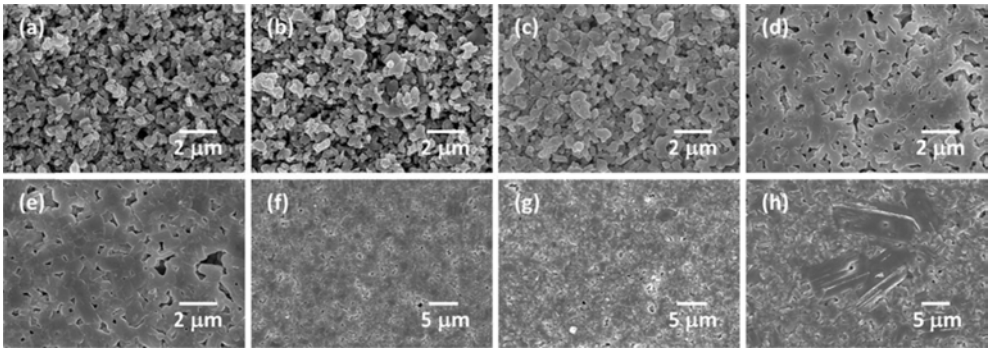

Fig. 2. SEM micrographs of $BaFe_{12}O_{19}$ samples sintered for 1 hr at (a) 900 ºC; (b) 950 ºC; (c) 1000 ºC; (d) 1050 ºC; (e) 1100 ºC; (f) 1150 ºC; (g) 1200 ºC and (h) 1250 ºC.

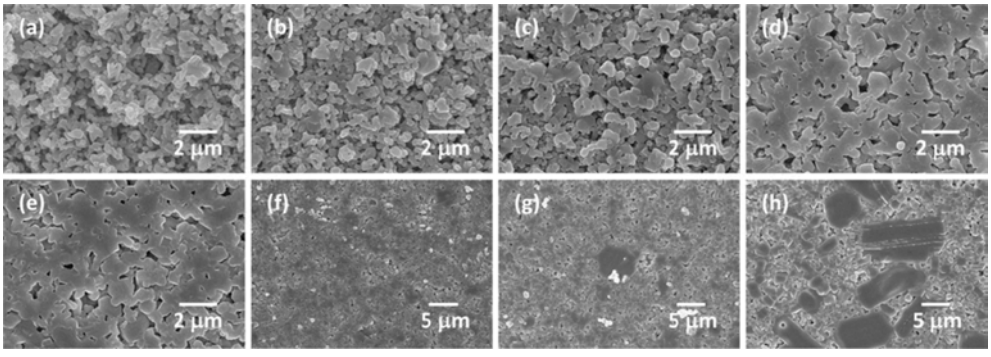

Fig. 3. SEM micrographs of 99 wt% $BaFe_{12}O_{19}$-1 wt% $CuWO_4$ samples sintered for 1 hr at (a) 900 ºC; (b) 950 ºC; (c) 1000 ºC; (d) 1050 ºC; (e) 1100 ºC; (f) 1150 ºC; (g) 1200 ºC and (h) 1250 ºC.

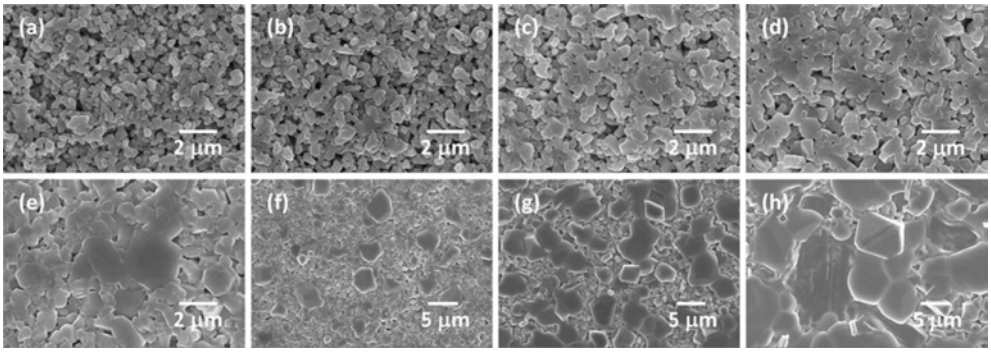

Fig. 4. SEM micrographs of 97 wt% $BaFe_{12}O_{19}$-3 wt% $CuWO_4$ samples sintered for 1 hr at (a) 900 ºC; (b) 950 ºC; (c) 1000 ºC; (d) 1050 ºC; (e) 1100 ºC; (f) 1150 ºC; (g) 1200 ºC and (h) 1250 ºC.

Table 1. Unit cell parameters of samples sintered at 1250 ºC for 1 hr.

Sample	a unit cell parameter (nm)	c unit cell parameter (nm)	Unit cell volume (nm^3)
$BaFe_{12}O_{19}$	0.589246 (0.0000369)	2.325636 (0.0002638)	0.6993
99 wt% $BaFe_{12}O_{19}$-1 wt% $CuWO_4$	0.588982 (0.000027)	2.321556 (0.0001774)	0.69745
97 wt% $BaFe_{12}O_{19}$-3 wt% $CuWO_4$	0.589001 (0.0000113)	2.323836 (0.0000661)	0.69818

the intermediate stage of sintering. Grain boundaries have formed between the particles but extensive interconnected porosity still exists. Samples sintered at ≥ 1150 ºC are in the final stage of sintering, with isolated pores between the grains. The samples sintered at 1150 ºC and 1200 ºC are in the initial stage of abnormal grain growth, with some grains ~3-6 μm in diameter. The sample sintered at 1250 ºC contains abnormal grains up to 20 μm in diameter. The sample sintered at 1250 ºC has some secondary phases present in the abnormal grains. The EDS analysis reveals this secondary phase to be Ba-deficient compared to the abnormal grains and matrix grains.

SEM micrographs of the 99 wt% $BaFe_{12}O_{19}$-1 wt% $CuWO_4$ samples sintered at temperatures between 900-1250 ºC for 1 h are shown in Fig. 3. The microstructure is very similar to that of the $BaFe_{12}O_{19}$ samples. Abnormal grain growth has also taken place in the samples sintered at 1150 ºC, 1200 ºC and 1250 ºC. White-coloured particles of a secondary phase appear to be visible. However, EDS analysis of this phase shows it to be $BaFe_{12}O_{19}$.

SEM micrographs of the 97 wt% $BaFe_{12}O_{19}$-3 wt% $CuWO_4$ samples sintered at temperatures between 900-1250 ºC for 1 hr are shown in Fig. 4. The samples sintered at 900-1050 ºC have microstructures similar to those of the $BaFe_{12}O_{19}$ and 99 wt% $BaFe_{12}O_{19}$-1 wt% $CuWO_4$ samples. What appear to be abnormal grains are present in the sample sintered at 1100 ºC [Fig. 4 (e)]. However, EDS analysis of these grains shows them to be FeO or Fe_2O_3. Large grains appear in the sample sintered at 1150 ºC [Fig. 4 (f)]. EDS analysis shows these grains to be $BaWO_4$ secondary phase. These secondary phase particles also contain 3-7 at. % Fe. As the sintering temperature increases further, the amount of $BaWO_4$ second phase also increases. In the

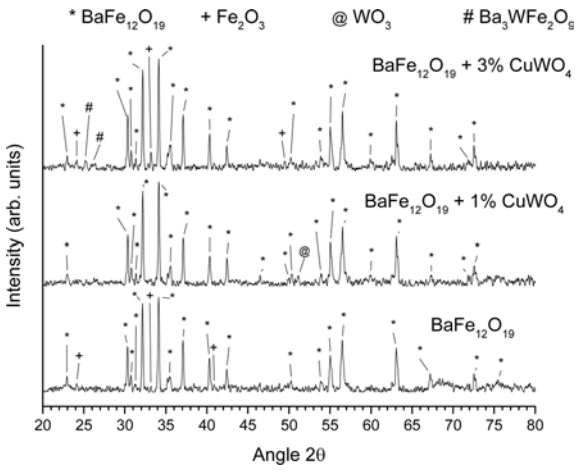

Fig. 5. XRD patterns of $BaFe_{12}O_{19}$, 99 wt% $BaFe_{12}O_{19}$-1 wt% $CuWO_4$ and 97 wt% $BaFe_{12}O_{19}$-3 wt% $CuWO_4$ samples sintered at 1250 ºC for 1 hr.

sample sintered at 1250 ºC, triangular and octahedral grains of Fe_2O_3 secondary phase are also present. The Fe_2O_3 secondary phase contains 3-6 at. % Cu. EDS analysis of the $BaFe_{12}O_{19}$ matrix grains shows them to contain small amounts (< 1 at. %) of Cu and W. Abnormal grain growth of $BaFe_{12}O_{19}$ has also taken place.

XRD patterns of the $BaFe_{12}O_{19}$, 99 wt% $BaFe_{12}O_{19}$-1 wt% $CuWO_4$ and 97 wt% $BaFe_{12}O_{19}$-3 wt% $CuWO_4$ samples sintered at 1250 ºC for 1 hr are shown in Fig. 5. All the patterns can be indexed with ICDD card number 84-0757 for $BaFe_{12}O_{19}$. A small amount of Fe_2O_3 secondary phase (ICDD card number 87-1166) is present in the $BaFe_{12}O_{19}$ sample. A small amount of WO_3 secondary phase (ICDD card number 87-2397) may be present in the 99 wt% $BaFe_{12}O_{19}$-1 wt%

Table 2. Magnetic properties of samples sintered at 1250 °C for 1 hr.

Sample	In-plane saturation magnetization M_s (Am^2kg^{-1})	In-plane remanent magnetization M_r (Am^2kg^{-1})	In-plane coercivity H_c (kAm^{-1})
$BaFe_{12}O_{19}$	55	23	92.8
99 wt% $BaFe_{12}O_{19}$-1 wt% $CuWO_4$	52	19	83.9
97 wt% $BaFe_{12}O_{19}$-3 wt% $CuWO_4$	40	13	71.3

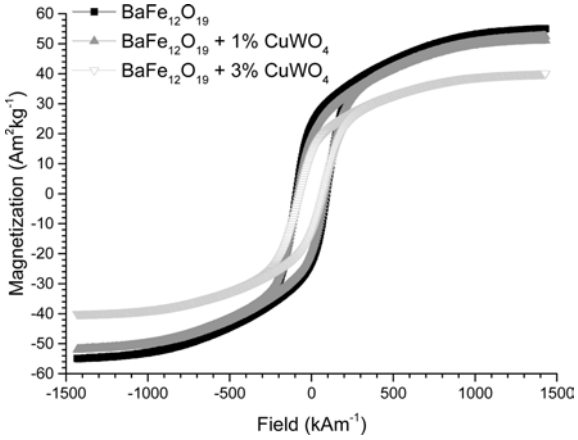

Fig. 6. In-plane M-H hysteresis loops of $BaFe_{12}O_{19}$, 99 wt% $BaFe_{12}O_{19}$-1 wt% $CuWO_4$ and 97 wt% $BaFe_{12}O_{19}$-3 wt% $CuWO_4$ samples sintered for 1 hr at 1250 °C.

$CuWO_4$ sample. Fe_2O_3 secondary phase is present in increased amounts in the 97 wt% $BaFe_{12}O_{19}$-3 wt% $CuWO_4$ sample. A small amount of $Ba_3WFe_2O_9$ (ICDD card number 74-1268) is present in the 97 wt% $BaFe_{12}O_{19}$-3 wt% $CuWO_4$ sample. The $BaWO_4$ phase visible in the SEM micrographs of the 97 wt% $BaFe_{12}O_{19}$-3 wt% $CuWO_4$ samples is not visible in the corresponding XRD pattern. The unit cell parameters of the samples are shown in Table 1. Addition of 1 wt % $CuWO_4$ causes a small decrease in the unit cell parameters of $BaFe_{12}O_{19}$, with further addition causing a small increase.

In-plane magnetization-field (M-H) hysteresis loops of samples sintered at 1250 °C for 1 hr are shown in Fig. 6. The magnetic properties are shown in Table 2. The M-H loops of all of the samples are typical of a hard ferrimagnetic material. Addition of 1 wt % $CuWO_4$ causes a decrease in saturation magnetization and remanent magnetization. Coercivity is also reduced. Addition of 3 wt % $CuWO_4$ causes a considerable decrease in saturation magnetization and remanent magnetization. Coercivity is further reduced.

Discussion

The addition of 1 wt% $CuWO_4$ has little effect on the sintering behavior at temperatures < 1050 °C, even though $CuWO_4$ is expected to melt at 1000 °C to form a liquid phase. The amount of $CuWO_4$ added is insufficient to affect the sintering behavior. From the XRD and VSM results, $CuWO_4$ may form a limited solid solution with $BaFe_{12}O_{19}$ at higher sintering temperatures (Table 1 and Table 2). The incorporation of Cu^{2+} and W^{6+} into the $BaFe_{12}O_{19}$ crystal lattice may affect lattice and grain boundary diffusion coefficients, which would affect the sintering behavior and may explain the reduced densification at higher sintering temperatures [11].

Addition of 3 wt % $CuWO_4$ promotes the sintering behavior at temperatures < 1100 °C. CuO-based liquid phase sintering aids were previously found to be effective in lowering the sintering temperature of $BaFe_{12}O_{19}$ [4, 8]. From the SEM and XRD results (Fig. 4 and Fig. 5), $CuWO_4$ is reacting with $BaFe_{12}O_{19}$ at temperatures > 1100 °C to form secondary phases of $BaWO_4$, $Ba_3WFe_2O_9$ and Fe_2O_3, probably by the following reactions:

$$BaFe_{12}O_{19} + CuWO_4 \rightarrow BaWO_4 + 6Fe_2O_3 + CuO \quad (1)$$

$$3BaFe_{12}O_{19} + CuWO_4 \rightarrow Ba_3WFe_2O_9 + 5Fe_2O_3 + CuO + \uparrow 18\ O_2(g) \quad (2)$$

From the EDS results, the CuO formed by these reactions is then forming a solid solution with Fe_2O_3. The changes in unit cell parameters indicate that some of the CuO may also form a solid solution with $BaFe_{12}O_{19}$ (Table 1). Hence the $CuWO_4$ acts as a liquid phase sintering aid only at lower sintering temperatures, reacting with $BaFe_{12}O_{19}$ to form secondary phases at higher temperatures. From the SEM micrographs (Fig. 4), reaction (1) begins at 1150 °C, which may explain the decrease in density in the 97 wt% $BaFe_{12}O_{19}$-3 wt% $CuWO_4$ samples compared to the $BaFe_{12}O_{19}$ samples.

The 12 Fe^{3+} ions in the $BaFe_{12}O_{19}$ formula unit are distributed over nine octahedral sites (co-ordination number CN = 6), two tetrahedral sites (CN = 4) and one trigonal bi-pyramidal site (CN = 5) [1, 2]. From Shannon [12], the ionic radii of Fe^{3+} are 0.49 Å (CN = 4), 0.58 Å (CN = 5), and 0.645 Å (CN = 6). The ionic radii of Cu^{2+} are 0.57 Å (CN = 4), 0.65 Å (CN = 5), and 0.73 Å (CN = 6). The ionic radii of W^{6+} are 0.42 Å (CN = 4), 0.51 Å (CN = 5), and 0.60 Å (CN = 6). Cu^{2+} and W^{6+} would be expected to replace Fe^{3}+ ions in the $BaFe_{12}O_{19}$ crystal lattice due to their similar size. However, the very small changes in unit cell parameters and unit cell volume indicate that little substitution takes place. The EDS results also showed

that only limited solid solution formation of Cu and W with $BaFe_{12}O_{19}$ took place. Addition of CuO was previously found to reduce the remanent magnetization of $BaFe_{12}O_{19}$ [4]. When Cu^{2+} substitutes for Fe^{3+} in the crystal lattice, the lower number of unpaired d-shell electrons (one compared to five for Fe^{3+}) reduces the magnetic moment. A comparison of ionic radii indicates that W^{6+} would also substitute for Fe^{3+} in the crystal lattice, although the degree of substitution would be limited due to the charge difference [12]. W^{6+} would have no unpaired d-shell electrons, so substitution for Fe^{3+} would be expected to reduce the magnetic moment still further. The 99 wt% $BaFe_{12}O_{19}$-1 wt% $CuWO_4$ sample does show reduced saturation and remanent magnetization (Table 2) indicating that some substitution of Fe^{3+} by Cu^{2+} and W^{6+} has taken place. The 97 wt% $BaFe_{12}O_{19}$-3 wt% $CuWO_4$ sample shows a larger reduction in saturation and remanent magnetization, due to the reaction of $BaFe_{12}O_{19}$ with $CuWO_4$ to produce Fe_2O_3, which is antiferromagnetic or weakly ferromagnetic [13].

Conclusions

The use of $CuWO_4$ as a liquid phase sintering aid for $BaFe_{12}O_{19}$ is studied. Compared to $BaFe_{12}O_{19}$ with no sintering aid addition, addition of 1 wt % $CuWO_4$ retards densification. Addition of 3 wt % promotes densification at temperatures below 1100 ºC but retards it at higher sintering temperatures. $CuWO_4$ reacts with $BaFe_{12}O_{19}$ at temperatures ≥ 1150 ºC to form Fe_2O_3, $BaWO_4$ and $Ba_3WFe_2O_9$ secondary phases. Samples sintered at 1250 ºC show hysteresis loops typical of a hard ferrimagnetic material. Addition of 1 wt% $CuWO_4$ causes a decrease in saturation and remanent magnetization. Addition of 3 wt% $CuWO_4$ causes a more severe decrease in saturation and remanent magnetization as well as coercivity, due to the formation of secondary phases. Based on these results, $CuWO_4$ is not suitable as a liquid phase sintering aid for $BaFe_{12}O_{19}$.

Acknowledgments

This research was supported by the Basic Science Research Program through the National Research Foundation of Korea (NRF), funded by the Ministry of Education (grant number: 2015R1D1A1A01057060). The authors would like to thank Dr. Seok Bae (LG Innotek) for providing the $BaFe_{12}O_{19}$ powder, Kyeong-Kap Jeong (Center for Research Facilities, Chonnam National University) for operating the XRD, Hey-Jeong Kim for operating the SEM, and Prof. Byong-Guk Park (KAIST) for carrying out the VSM measurements.

References

1. A.J. Moulson and J.M. Herbert, in "Electroceramics: Materials, Properties, Applications. 2nd Edition" (John Wiley & Sons Ltd., 2003) pp. 469-546.
2. G. Alex, in "Modern Ferrite Technology" (Springer, 2010) pp. 51-70.
3. J. Jalli, Y.-K. Hong, S. Bae, J.-J. Lee, G.S. Abo, A. Lyle, S.-H. Gee, H. Lee, T. Mewes, J.-C. Sur and S.-I. Lee, J. Appl. Phys. 105[7] (2009) 07A511.
4. H. Vu, D. Nguyen, J.G. Fisher, W.-H. Moon, S. Bae, H.-G. Park and B.-G. Park, Journal of Asian Ceramic Societies 1[2] (2013) 170-177.
5. M. Hagymási, A. Roosen, R. Karmazin, O. Dernovsek and W. Haas, J. Eur. Ceram. Soc. 25[12] (2005) 2061-2064.
6. V.A. Rane, G.J. Phatak and S.K. Date, IEEE Trans. Magn. 49[9] (2013) 5048-5054.
7. Y. Wang, Y.L. Liu, J. Li, Q. Liu, H.W. Zhang and V.G. Harris, AIP Adv. 6[5] (2016) 7.
8. C. Wu, Z. Yu, G. Wu, K. Sun, Y. Yang, X. Jiang, R. Guo and Z. Lan, IEEE Trans. Magn. 51[11] (2015) 1-4.
9. J.B. Forsyth, C. Wilkinson and A.I. Zvyagin, J. Phys.: Condens. Matter 3[43] (1991) 8433.
10. T.N. Kol'tsova and G.D. Nipan, Inorg. Mater. 35[4] (1999) 383-384.
11. S.J.L. Kang, in "Sintering: Densification, Grain Growth & Microstructure" (Elsevier Butterworth Heinemann, 2005) pp. 181-192.
12. R.D. Shannon, Acta Crystallographica Section A 32[5] (1976) 751-767.
13. R.N. Bhowmik and A. Saravanan, J. Appl. Phys. 107[5] (2010) 053916.